AGU PUBLICATIONS

Geophysical Research Letters

RESEARCH LETTER

10.1002/2015GL063874

Key Points:
- Standard diffusion codes overestimate pitch angle scattering at small angles
- Relative importance of nonresonant interactions
- Quantitative important mismatches between PIC and diffusion simulations

Correspondence to:
E. Camporeale,
e.camporeale@cwi.nl

Citation:
Camporeale, E. (2015), Resonant and nonresonant whistlers-particle interaction in the radiation belts, *Geophys. Res. Lett.*, *42*, 3114–3121, doi:10.1002/2015GL063874.

Received 16 MAR 2015
Accepted 3 APR 2015
Accepted article online 9 APR 2015
Published online 7 MAY 2015

Resonant and nonresonant whistlers-particle interaction in the radiation belts

Enrico Camporeale[1]

[1] Center for Mathematics and Computer Science (CWI), Amsterdam, Netherlands

Abstract We study the wave-particle interactions between lower band chorus whistlers and an anisotropic tenuous population of relativistic electrons. We present the first direct comparison of first-principle particle-in-cell (PIC) simulations with a quasi-linear diffusion code. In the PIC approach, the waves are self-consistently generated by the temperature anisotropy instability that quickly saturates and relaxes the system toward marginal stability. We show that the quasi-linear diffusion and PIC results have significant quantitative mismatch in regions of energy/pitch angle where the resonance condition is not satisfied. Moreover, for pitch angles close to the loss cone the diffusion code overestimates the scattering, particularly at low energies. This suggests that higher-order nonlinear theories should be taken in consideration in order to capture nonresonant interactions, resonance broadening, and to account for scattering at angles close to 90°.

1. Introduction

Resonant wave-particle interactions play a fundamental role in space plasma physics. In the radiation belts, energetic electrons that are potentially harmful to satellites are subject to pitch angle scattering and local acceleration due to cyclotron and Landau resonances [*Thorne*, 2010; *Summers et al.*, 2013]. The nonconservation of the adiabatic invariants of motion leads to detrapping and to scattering into the loss cone, where particles eventually precipitate into the ionosphere. The accurate prediction of the time scale associated with the loss mechanisms of such energetic particles still represents a major challenge, in a space weather perspective.

The standard theoretical framework for the modeling of wave-particle interactions is based on quasi-linear theory, initially developed in the seminal paper by *Kennel and Engelmann* [1966] and broadly used in the context of cosmic ray acceleration [*Jokipii*, 1966; *Kulsrud and Pearce*, 1969; *Schlickeiser*, 1989], tokamaks [*Hazeltine et al.*, 1981], and radiation belt physics [*Lyons et al.*, 1972; *Summers et al.*, 1998]. The quasi-linear procedure describes wave-particle interactions by means of a diffusion equation in pitch angle and energy for the particle distribution function, by expanding particle orbits around their unperturbed trajectory in the Vlasov-Maxwell equations [*Swanson*, 2012]. The complexity of wave-particle interactions is thus dramatically reduced to a diffusive process, and all the physical information is lumped into the diffusion coefficients, usually defined as a function of particles' pitch angle and energy. Following the quasi-linear paradigm, the derivation and numerical calculation of diffusion coefficients for several kinds of plasma waves have been the focus of a great part of radiation belt physics in recent years [*Albert and Young*, 2004; *Summers*, 2005; *Glauert and Horne*, 2005; *Shprits et al.*, 2006; *Mourenas and Ripoll*, 2012]. Multidimensional diffusion codes have proved quite successful in studying the time evolution of the electron distribution function before, during, and after a storm [*Thorne et al.*, 2013; *Tu et al.*, 2013; *Miyoshi et al.*, 2006; *Jordanova et al.*, 2010; *Fok et al.*, 2008; *Tao et al.*, 2009; *Varotsou et al.*, 2008; *Albert et al.*, 2009; *Shprits et al.*, 2009; *Subbotin and Shprits*, 2009; *Tu et al.*, 2009; *Xiao et al.*, 2009, 2010; *Su et al.*, 2011]. Moreover, quasi-linear diffusion coefficients have recently been compared to results from test particle simulations. *Tao et al.* [2011] made this comparison for whistler mode chorus and *Liu et al.* [2010] for electromagnetic ion cyclotron waves. Both found an excellent agreement. *Tao et al.* [2012] have also reported the breakdown of the quasi-linear theory predictions when, as expected, the wave amplitude is sufficiently large.

It is important to remind that the resonant quasi-linear theory employed in radiation belt studies is based on the following three approximations: the waves have random phase and small amplitude, and the particles are in (either cyclotron or Landau) resonance with the wave spectrum [*Lemons*, 2012]. Although not strictly required, most quasi-linear calculations have been carried over by assuming a spectrum of waves derived by

the cold plasma linear theory, i.e., neglecting thermal effects. Wave damping/growth is generally neglected, since it increases the complexity of the derivation of the diffusion coefficients. Finally, an accurate calculation of the diffusion coefficient requires the detailed information on the wave power spectrum, which is generally assumed as a Gaussian centered around a dominant mode [*Horne et al.*, 2005].

In this paper, we present particle-in-cell (PIC) simulations and we focus on the wave-particle interactions between energetic electrons and whistlers generated by an anisotropic suprathermal relativistic population. With such approach the wave spectrum is self-consistently generated and no further assumptions are required. The resonant interactions between particles and a wave field that is growing in time due to an ongoing kinetic instability have not been studied before in a self-consistent way. We present, for the first time, a quantitative comparison between PIC and Fokker-Planck simulations. In this way we can directly assess the range of validity of the standard quasi-linear approach and its drawbacks. It is worth noting that in the cosmic ray acceleration context, several authors have highlighted the weaknesses of standard quasi-linear diffusion, leading to the development of second-order quasi-linear theory and weakly nonlinear theory [see, e.g., *Shalchi and Schlickeiser*, 2005; *Qin and Shalchi*, 2009], where the particle orbit calculation takes in account the electromagnetic perturbation. In particular, the standard quasi-linear theory fails to predict the correct scattering for large pitch angles ("the 90° problem") [*Tautz et al.*, 2008]. More recently, *Ragot* [2012] has questioned the relative importance between resonant and nonresonant interactions in a turbulent magnetized plasma. Finally, it is important to emphasize that one of the most relevant quantities for space weather predictions is the particle lifetime. A standard estimate is based on the inverse of the bounce-averaged diffusion coefficient evaluated at the equatorial loss cone angle, for different energies [*Shprits et al.*, 2006]. Such estimate has been validated in *Albert and Shprits* [2009] and parametrized in *Shprits et al.* [2007]. The electron loss time scale varies from a few hours to a few days depending on the latitude distribution of wave power, the energy, and the cold plasma parameter $\alpha^* = \Omega_e^2/\omega_p^2$ (with ω_p and Ω_e the electron plasma and equatorial cyclotron frequency, respectively). However, we will show that quasi-linear diffusion tends to overestimate diffusion rates at small pitch angles: this important result suggests to reconsider the standard estimates of particle lifetime.

We focus on the physics of whistler waves, which are routinely observed in the magnetosphere and are believed to play a dominant role for relativistic electron acceleration and precipitation [*Horne and Thorne*, 2003]. Whistler waves can be generated by man-made VLF transmissions [*Dungey*, 1963] or as the result of anisotropic plasma injection during a magnetic storm [*Jordanova et al.*, 2010]. Indeed, equatorial whistler mode chorus can be excited by cyclotron resonance with anisotropic 10–100 KeV electrons injected from the plasma sheet [*Summers et al.*, 2007]. A statistical analysis of chorus excitation observed by THEMIS has recently been presented by *Li et al.* [2010]. They have reported dayside lower band chorus generated by anisotropic 10–100 KeV electrons. The superposed epoch analysis during geomagnetic storms performed at GEO orbit by *MacDonald et al.* [2008] suggests that whistler wave growth is related to relativistic electron enhancements, but they have not found instances where the whistler marginal stability condition is actually reached, thus suggesting that the anisotropic suprathermal population is seldom strongly unstable, but rather in a condition of marginal stability. Indeed, the long-standing scenario envisioned for radiation belt electrons implies a delicate equilibrium between losses due to pitch angle scattering into the loss cone and enhanced wave activity due to kinetic instabilities triggered by anisotropic loss cone distributions [*Lyons and Thorne*, 1973].

2. Methodology

We present one-dimensional particle-in-cell (PIC) simulations performed with the implicit code Parsek2D [*Markidis et al.*, 2009, 2010]. In order to simulate a situation relevant to the lower band chorus generation in the radiation belt, we have chosen the following parameters. The background homogeneous magnetic field is $B_0 = 4 \cdot 10^{-7} T$, corresponding to the equatorial value at $L \sim 4.3$, and it is aligned with the box (the assumption of homogeneous field is justified because the time scale of the simulation is much shorter than the bounce period).

The electron population has a density of 15 cm^{-3} (the resulting cold plasma parameter is $\alpha^* = 0.104$), and it is composed for 98.5% by a cold isotropic Maxwellian (1 eV) and for 1.5% by an anisotropic relativistic bi-Maxwellian distribution $f(v_{||}, v_\perp) \sim \exp\left[-\alpha_\perp \gamma - (\alpha_{||} - \alpha_\perp)\gamma_{||}\right]$ (with $\gamma = (1-v^2/c^2)^{-1/2}$, $\gamma_{||} = (1-v_{||}^2/c^2)^{-1/2}$, and parallel and perpendicular refer to the background magnetic field) [*Naito*, 2013; *Davidson and Yoon*, 1989]. We choose $\alpha_{||} = 25$ and $\alpha_\perp = 4$. The hot electrons velocity distribution function has standard deviations

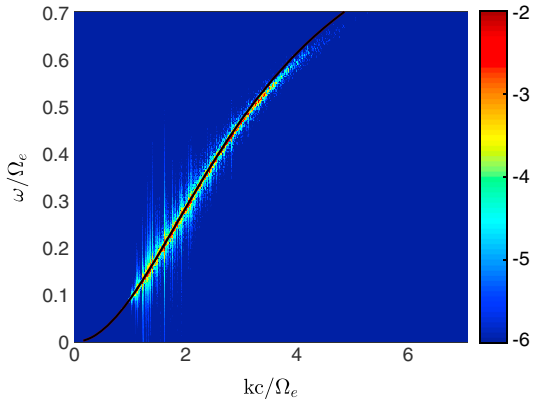

Figure 1. Spectrogram of magnetic fluctuations, in logarithmic scale. The black line shows the cold plasma dispersion relation. Most of the wave power is confined to $\omega \lesssim 0.5\Omega_e$.

$\sqrt{\langle v_{||}^2 \rangle} = 0.175$ and $\sqrt{\langle v_{\perp}^2 \rangle} = 0.325$ (normalized to speed of light) corresponding to nominal temperatures of 8 KeV and 30 KeV, respectively. Thus, the initial anisotropy of the suprathermal component is $T_\perp/T_{||} = 3.75$. We note that in order to accurately recover the quasi-linear pitch angle diffusion, one has to ensure that the wave vector separation $\Delta k = 2\pi/L$ is small enough, such that each particle is subject to a relatively broad spectrum of modes. In our simulations the box length $L = 400c/\Omega_e$ and the most dominant modes have wavelength of about 1/200 of the box length. The number of grid points is 8000. The diffusion code employed in this paper is described in *Camporeale et al.* [2013]. We solve the nonbounce-averaged Fokker-Planck equation in energy and pitch angle on a computational box $[0°, 89.9°] \times [10, 500]$ KeV, with diffusion coefficients evaluated as in *Summers* [2005]. Mixed energy/pitch angle diffusion is included. The boundary conditions are $f(t) = f(t = 0)$ at the lower and higher-energy boundaries and for 0° pitch angle. A Neumann condition $\mathrm{d}f/\mathrm{d}\alpha = 0$ is used at the 89.9° boundary.

3. Results

In Figure 1, we show the spectrogram of the magnetic fluctuations from PIC simulations, in logarithmic scale. By virtue of the one-dimensional setup, the fluctuations are perpendicular to the background field. The black line shows the cold plasma dispersion relation for equal parameters but without the suprathermal component, which is in very good agreement. Note that most of the wave power is confined to $\omega/\Omega_e \lesssim 0.5$. It is well known that temperature anisotropy instabilities have a "self-destructing" character, in the sense that the generated electromagnetic fluctuations reduce the anisotropy that drives the instability, and therefore, a marginal stability condition is usually rapidly reached [*Camporeale and Burgess*, 2008; *Gary et al.*, 2014]. This effect is shown in Figure 2. Electromagnetic energy (left axis) and anisotropy $T_\perp/T_{||}$ (right axis) are plotted as a function of time in electron gyroperiod units. The reduction of anisotropy is indeed very strongly correlated to the linear growth phase of the instability, roughly for $T\Omega_e < 1000$. The linear instability saturates at a large-amplitude $\delta B/B_0 \sim 10\%$, and thus, in the postsaturation regime the quasi-linear theory might not be applicable.

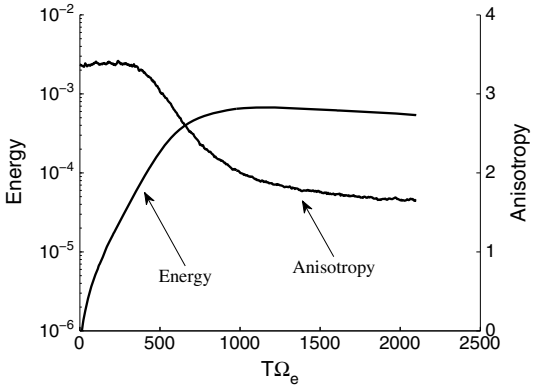

Figure 2. Time development of energy (left axes, logarithmic scale) and temperature anisotropy $T_\perp/T_{||}$ (right axes, linear scale). Time is normalized to electron gyrofrequency.

3.1. Resonance Curves

Before commenting on the comparison between PIC and diffusion code results, it is useful to briefly revise a few basic concepts concerning wave-particle resonance and resonance curves. A particle is in resonance with a wave with frequency ω and wave vector k if the following relation is satisfied:

$$\omega - kv\cos\alpha = n\Omega_e\sqrt{1 - v^2/c^2}, \quad (1)$$

which simply means that the relativistic gyrofrequency of the particle matches the Doppler-shifted wave

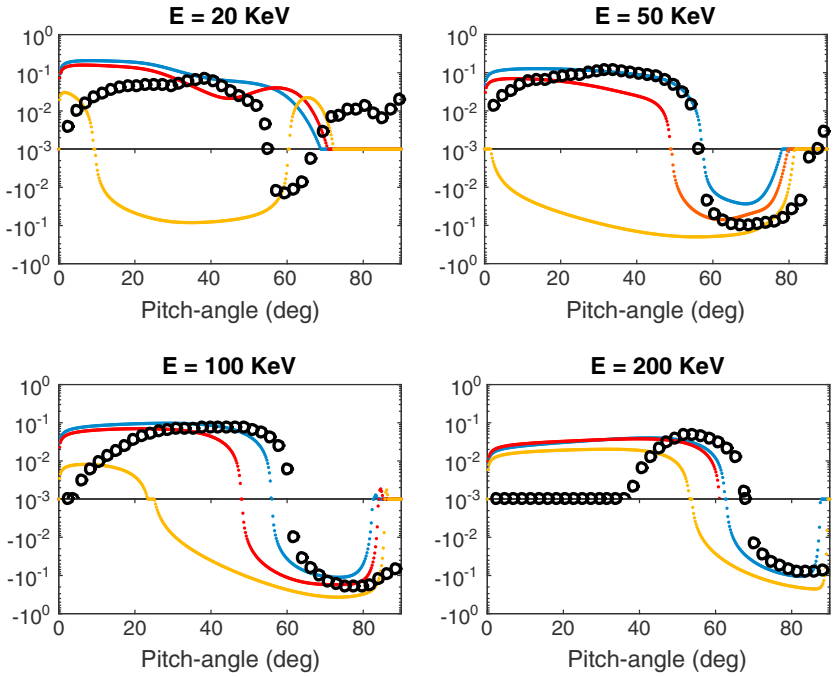

Figure 3. Comparison between PIC and diffusion code results. Difference in the probability density functions between time $T\Omega_e = 1000$ and initial condition, for energies $E = 20$, 50, 100, and 200 KeV, as function of pitch angle α (in degrees). Blue, red, and yellow lines show the results from diffusion code, with $\delta B/B_0 = 1\%$, 2%, and 5%, respectively. Black circles are for PIC results. The vertical axes are in logarithmic scale (with sign), with a cutoff at 10^{-3}.

frequency. The order of resonance $n = 0$ and $n = 1, 2, \ldots$ is respectively for Landau and cyclotron resonances. Equation (1) shows resonance curves, which are ellipses in $(v_{||}, v_{\perp})$ space on which the resonance condition is satisfied. If the wave is confined within a certain range of frequencies (and wave vectors), as it is the case here (see Figure 1), equation (1) can be used to calculate the minimum energy that is required for a particle with a given pitch angle α in order to satisfy the resonance condition. For this purpose, equation (1) can be rewritten, for $n = 1$, as

$$\cos\alpha = \frac{\omega_M(E+1)-1}{k\sqrt{E^2+2E}}, \tag{2}$$

where E is the relativistic energy normalized to the rest mass and ω_M the upper bound of the frequency range normalized to Ω_e. For completeness, we recall that the wave vector k can be calculated by using the cold plasma dispersion relation for whistler waves:

$$kc/\omega = \sqrt{1 - \frac{\omega_p^2/\Omega_e^2}{\omega(\omega-\Omega_e)}} \tag{3}$$

3.2. Comparison Between PIC and Diffusion Code

Since diffusion coefficients are very sensitive to the magnetic wave power spectrum (but actually not much to the exact shape of the spectrum), a comparison between PIC simulations and a diffusion code raises the question of which magnetic spectrum to choose, since this is evolving in time during the linear growth phase. We show results for three values of fluctuation amplitude: $\delta B/B_0 = 1\%$, 2%, and 5%. In the diffusion code, the fluctuating field amplitude does not change in time, and hence, it has to be interpreted as an effective time-averaged field amplitude. All the results are shown for time $T\Omega_e = 1000$, and we have verified that the mean value of $\delta B/B_0$ between times $T\Omega_e = 0$ and $T\Omega_e = 1000$ is approximately 5%. The values $\delta B/B_0 = 1\%$ and 2% occur when the average is performed until times $T\Omega_e = 300$ and 500, respectively. The PIC results suggest that it is reasonable to use a Gaussian spectrum centered at $\omega/\Omega_e = 0.2$, with semibandwidth equal to 0.25.

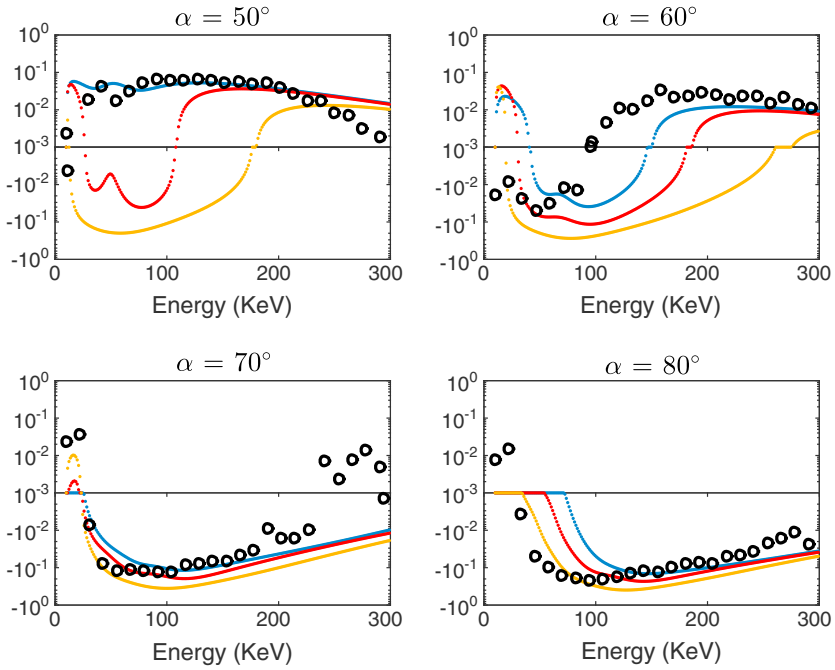

Figure 4. Comparison between PIC and diffusion code results. Difference in the probability density functions between time $T\Omega_e = 1000$ and initial condition, for pitch angles $\alpha = 50°$, 60°, 70°, and 80° as function of energy. Same legend as in Figure 3.

We show a direct comparison between PIC and diffusion codes, in terms of probability density function (pdf) of the suprathermal species. Of course, such quantity is readily available in PIC simulations, and the statistics is performed on 160,000 particles. However, for the results shown here, the pdf statistics degrades for energies above ~250 KeV.

Figures 3 and 4 show the difference between the pdf at time $T\Omega_e = 1000$ and the initial condition. PIC results are represented by circles, while the diffusion code results for $\delta B/B_0 = 1\%$, 2%, and 5% are shown in blue, red, and yellow, respectively. The vertical axes in Figures 3 and 4 are logarithmic, with a cutoff at 10^{-3}. In this way, we can show in a single plot the positive and negative parts of $f(t = 1000\Omega_e^{-1}) - f(t = 0)$, hence showing whether the diffusion enhances or depletes the distribution function. The pdfs are not normalized but rescaled such that its maximum value at initial time is equal to 1. Figure 3 shows the change in the pdfs as a function of pitch angle for energies $E = 20$, 50, 100, and 200 KeV. Three features are evident in Figure 3. First, the diffusion code overestimates the diffusion at small pitch angles. Indeed, there is at least an order of magnitude discrepancy between the diffusion code results and the PIC, for all energies, for pitch angles less than 10°. Second, the diffusion code does not capture scattering close to 90° pitch angle, which can instead be significant in the PIC. Third, for each energy, there is a range in pitch angles where the diffusion code does not predict any diffusion; i.e., the curves lie flat at the cutoff level 10^{-3}. This follows from the argument that we have presented above: particles need to have a sufficient energy in order to fulfill the resonance condition. This feature is even more evident in Figure 4. Here we show (with same legend as in Figure 3) the change in the pdf with respect to the initial condition as a function of energy for pitch angles $\alpha = 50°$, 60°, 70°, and 80°. No general trend is identifiable: the agreement between the codes is good in some regions but not everywhere. In particular, a large disagreement is noticeable for small energy and large pitch angles. Finally, in Figure 5 we present the two-dimensional color plots of the particle distribution functions for PIC (top left) and diffusion code (top right, $\delta B/B_0 = 1\%$), in logarithmic scale, at time $T\Omega_e = 1000$. Figure 5 (bottom) evidently emphasizes the downsides of the diffusion code. It shows the absolute value of the difference between the diffusion code and the PIC results (we remind that the distribution function values range between 0 and 1). The superposed black line denotes the minimal resonant energy for a given pitch angle, calculated via equation (2), by using a maximum frequency $\omega_M/\Omega_e = 0.5$. Very interestingly, for large pitch angles the larger mismatches lie below the black curve, where nonresonant scattering takes place and, as such, the diffusion code performs

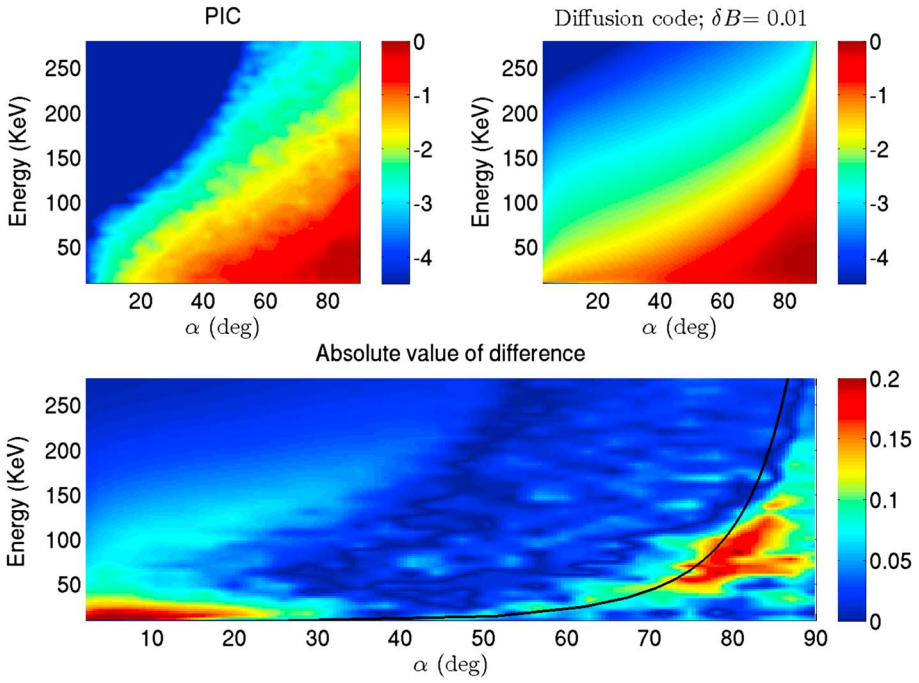

Figure 5. Comparison between PIC and diffusion code results. (top left) Probability density functions for PIC and (top right) diffusion code for the case $\delta B/B_0 = 1\%$, at time $T\Omega_e = 1000$. (bottom) The absolute value of the difference between the two solutions. Below the black line the resonant condition equation (1) requires $\omega/\Omega_e > 0.5$, and therefore, only nonresonant interactions are possible.

poorly. The small pitch angle region is also quantitatively different, with the larger mismatch for small energies. This indicates that the actual particle lifetime might be larger than the one estimated through the quasi-linear diffusion coefficients.

4. Discussion

We have presented a direct comparison between first-principle PIC and quasi-linear diffusive simulations. The focus has been on one-dimensional PIC simulations of wave-particle interactions between suprathermal electron and lower band chorus waves. In PIC, the waves are self-consistently generated by an initial small population of anisotropic energetic electrons. This approach does not require any of the assumptions used by quasi-linear theory or test particle simulations. We have initialized the suprathermal component with a bi-Maxwellian relativistic distribution. This might not be completely realistic, and future work will test the effects of kappa-type distributions, such as the one studied, e.g., in *Xiao* [2006] and *Xiao et al.* [2008]. The particle diagnostic has been performed on samples of 160,000 PIC particles, resulting in excellent statistics, for the energies considered. We have chosen a fixed value of $\delta B/B_0$, for the calculation of diffusion coefficients, and such value must be interpreted, in the diffusion code, as an effective time average. It is important to realize that the results for $\delta B/B_0 = 5\%$ produce the largest disagreement with respect to PIC, in Figures 3 and 4, although this is the value closer to the correct time average in the interval $T = 0$ to $T\Omega_e = 1000$. This suggests that when diffusion codes are used in conjunction with satellite data, the observed values of $\delta B/B_0$ might be misleading if the wave is subject to linear growth.

We have highlighted some important differences in the results from PIC and diffusion code. First, the quasi-linear code generally overestimates diffusion for small pitch angles. This is an important result that implies a reconsideration of the standard estimates of particle lifetime, which is usually based on the characteristic diffusion times at loss cone angles. Second, we have presented evidence of nonresonant wave-particle interactions at large pitch angles that, by construction, cannot adequately be described in the widely employed resonant limit of the quasi-linear theory. In this respect, it would be interesting to test higher-order nonlinear theories, such as the ones described in *Qin and Shalchi* [2009].

In conclusions, our PIC simulations corroborate the long-standing viewpoint that diffusion codes are a useful reduced model for the study of wave-particle interaction phenomena in the radiation belts, but at the same time, in view of more quantitative predictions, they solicit an effort to include nonresonant interactions.

Acknowledgments
Data used in this paper are available upon request to the author.

The Editor thanks two anonymous reviewers for their assistance in evaluating this paper.

References

Albert, J. M., and Y. Shprits (2009), Estimates of lifetimes against pitch angle diffusion, *J. Atmos. Sol. Terr. Phys.*, *71*(16), 1647–1652.

Albert, J. M., and S. L. Young (2004), Using quasi-linear diffusion to model acceleration and loss from wave-particle interactions, *Space Weather*, *2*, S09S03, doi:10.1029/2004SW000069.

Albert, J. M., N. P. Meredith, and R. B. Horne (2009), Three-dimensional diffusion simulation of outer radiation belt electrons during the 9 October 1009 magnetic storm, *J. Geophys. Res.*, *114*, A09214, doi:10.1029/2009JA014336.

Camporeale, E., and D. Burgess (2008), Electron firehose instability: Kinetic linear theory and two-dimensional particle-in-cell simulations, *J. Geophys. Res.*, *113*, A07107, doi:10.1029/2008JA013043.

Camporeale, E., G. Delzanno, S. Zaharia, and J. Koller (2013), On the numerical simulation of particle dynamics in the radiation belt: 1. Implicit and semi-implicit schemes, *J. Geophys. Res. Space Physics*, *118*(6), 3463–3475, doi:10.1002/jgra.50293.

Davidson, R. C., and P. H. Yoon (1989), Nonlinear bound on unstable field energy in relativistic electron beams and plasmas, *Phys. Fluids B*, *1*(1), 195–203.

Dungey, J. (1963), Loss of Van Allen electrons due to whistlers, *Planet. Space Sci.*, *11*(6), 591–595.

Fok, M.-C., R. B. Horne, N. P. Meredith, and S. A. Glauert (2008), Radiation Belt Environment model: Application to space weather nowcasting, *J. Geophys. Res.*, *113*, A03S08, doi:10.1029/2007JA012558.

Gary, S. P., R. S. Hughes, J. Wang, and O. Chang (2014), Whistler anisotropy instability: Spectral transfer in a three-dimensional particle-in-cell simulation, *J. Geophys. Res. Space Physics*, *119*(3), 1429–1434, doi:10.1002/2013JA019618.

Glauert, S. A., and R. B. Horne (2005), Calculation of pitch angle and energy diffusion coefficients with the PADIE code, *J. Geophys. Res.*, *110*, A04206, doi:10.1029/2004JA010851.

Hazeltine, R., S. Mahajan, and D. Hitchcock (1981), Quasi-linear diffusion and radial transport in tokamaks, *Phys. Fluids*, *24*(6), 1164–1179.

Horne, R., and R. Thorne (2003), Relativistic electron acceleration and precipitation during resonant interactions with whistler-mode chorus, *Geophys. Res. Lett.*, *30*(10), 1527, doi:10.1029/2003GL016973.

Horne, R. B., R. M. Thorne, S. A. Glauert, J. M. Albert, N. P. Meredith, and R. R. Anderson (2005), Timescale for radiation belt electron acceleration by whistler mode chorus waves, *J. Geophys. Res.*, *110*, A03225, doi:10.1029/2004JA010811.

Jokipii, J. (1966), Cosmic-ray propagation: I. Charged particles in a random magnetic field, *Astrophys. J.*, *146*, 480, doi:10.1086/148912.

Jordanova, V. K., R. M. Thorne, W. Li, and Y. Miyoshi (2010), Excitation of whistler mode chorus from global ring current simulations, *J. Geophys. Res.*, *115*, A00F10, doi:10.1029/2009JA014810.

Kennel, C., and F. Engelmann (1966), Velocity space diffusion from weak plasma turbulence in a magnetic field, *Phys. Fluids*, *9*(12), 2377–2388.

Kulsrud, R., and W. P. Pearce (1969), The effect of wave-particle interactions on the propagation of cosmic rays, *Astrophys. J.*, *156*, 445, doi:10.1086/149981.

Lemons, D. S. (2012), Pitch angle scattering of relativistic electrons from stationary magnetic waves: Continuous Markov process and quasilinear theory, *Phys. Plasmas*, *19*(1), 12306, doi:10.1063/1.3676156.

Li, W., et al. (2010), THEMIS analysis of observed equatorial electron distributions responsible for the chorus excitation, *J. Geophys. Res.*, *115*, A00F11, doi:10.1029/2009JA014845.

Liu, K., D. S. Lemons, D. Winske, and S. P. Gary (2010), Relativistic electron scattering by electromagnetic ion cyclotron fluctuations: Test particle simulations, *J. Geophys. Res.*, *115*, A04204, doi:10.1029/2009JA014807.

Lyons, L. R., and R. M. Thorne (1973), Equilibrium structure of radiation belt electrons, *J. Geophys. Res.*, *78*(13), 2142–2149.

Lyons, L. R., R. M. Thorne, and C. F. Kennel (1972), Pitch-angle diffusion of radiation belt electrons within the plasmasphere, *J. Geophys. Res.*, *77*(19), 3455–3474.

MacDonald, E., M. Denton, M. Thomsen, and S. Gary (2008), Superposed epoch analysis of a whistler instability criterion at geosynchronous orbit during geomagnetic storms, *J. Atmos. Sol. Terr. Phys.*, *70*(14), 1789–1796.

Markidis, S., E. Camporeale, D. Burgess, and G. Lapenta (2009), Parsek2d: An implicit parallel particle-in-cell code, in *Numerical Modeling of Space Plasma Flows: ASTRONUM-2008 ASP Conf. Ser., Proceedings of the Conference held 8-13 June, 2008 at The Westin Hotel, St. John, U.S. Virgin Islands*, vol. 406, edited by N. V. Pogorelov other, p. 237, Astron. Soc. of the Pacifc Conf., San Fracisco, Calif.

Markidis, S., G. Lapenta, and Rizwan-uddin (2010), Multi-scale simulations of plasma with IPIC3D, *Math. Comput. Simul.*, *80*(7), 1509–1519.

Miyoshi, Y. S., V. K. Jordanova, A. Morioka, M. F. Thomsen, G. D. Reeves, D. S. Evans, and J. C. Green (2006), Observations and modeling of energetic electron dynamics during the October 2001 storm, *J. Geophys. Res.*, *111*, A11S02, doi:10.1029/2005JA011351.

Mourenas, D., and J.-F. Ripoll (2012), Analytical estimates of quasi-linear diffusion coefficients and electron lifetimes in the inner radiation belt, *J. Geophys. Res.*, *117*, A01204, doi:10.1029/2011JA016985.

Naito, O. (2013), *Phys. Plasmas*, *20*(4), 44,501, doi:10.1063/1.4801036.

Qin, G., and A. Shalchi (2009), Pitch-angle diffusion coefficients of charged particles from computer simulations, *Astrophys. J.*, *707*(1), 61, doi:10.1088/0004-637X/707/1/61.

Ragot, B. (2012), Pitch-angle scattering: Resonance versus nonresonance, a basic test of the quasilinear diffusive result, *Astrophys. J.*, *744*(1), 75, doi:10.1088/0004-637X/744/1/75.

Schlickeiser, R. (1989), Cosmic-ray transport and acceleration. I—Derivation of the kinetic equation and application to cosmic rays in static cold media. II—Cosmic rays in moving cold media with application to diffusive shock wave acceleration, *Astrophys. J.*, *336*, 243–293.

Shalchi, A., and R. Schlickeiser (2005), Evidence for the nonlinear transport of galactic cosmic rays, *Astrophys. J. Lett.*, *626* (2), L97, doi:10.1086/431905.

Shprits, Y. Y., R. M. Thorne, R. B. Horne, and D. Summers (2006), Bounce-averaged diffusion coefficients for field-aligned chorus waves, *J. Geophys. Res.*, *111*, A10225, doi:10.1029/2006JA011725.

Shprits, Y. Y., N. P. Meredith, and R. M. Thorne (2007), Parameterization of radiation belt electron loss timescales due to interactions with chorus waves, *Geophys. Res. Lett.*, *34*, L11110, doi:10.1029/2006GL029050.

Shprits, Y. Y., L. Chen, and R. M. Thorne (2009), Simulations of pitch angle scattering of relativistic electrons with MLT-dependent diffusion coefficients, *J. Geophys. Res.*, *114*, A03219, doi:10.1029/2008JA013695.

Su, Z., H. Zheng, L. Chen, and S. Wang (2011), Numerical simulations of storm-time outer radiation belt dynamics by wave-particle interactions including cross diffusion, *J. Atmos. Sol. Terr. Phys.*, *73*, 95–105, doi:10.1016/j.jastp.2009.08.002.

Subbotin, D. A., and Y. Y. Shprits (2009), Three-dimensional modeling of the radiation belts using the Versatile Electron Radiation Belt (VERB) code, *Space Weather*, *7*, S10001, doi:10.1029/2008SW000452.

Summers, D. (2005), Quasi-linear diffusion coefficients for field-aligned electromagnetic waves with applications to the magnetosphere, *J. Geophys. Res.*, *110*, A08213, doi:10.1029/2005JA011159.

Summers, D., R. M. Thorne, and F. Xiao (1998), Relativistic theory of wave-particle resonant diffusion with application to electron acceleration in the magnetosphere, *J. Geophys. Res.*, *103*(A9), 20,487–20,500.

Summers, D., B. Ni, and N. P. Meredith (2007), Timescales for radiation belt electron acceleration and loss due to resonant wave-particle interactions: 1. Theory, *J. Geophys. Res.*, *112*, A04206, doi:10.1029/2006JA011801.

Summers, D., I. R. Mann, and D. N. Baker (2013), *Dynamics of the Earth's Radiation Belts and Inner Magnetosphere*, Wiley, Washington, D. C.

Swanson, D. G. (2012), *Plasma Waves,* 2nd ed., Inst. of Phys., Bristol, U. K., and Philadelphia, Pa.

Tao, X., J. M. Albert, and A. A. Chan (2009), Numerical modeling of multidimensional diffusion in the radiation belts using layer methods, *J. Geophys. Res.*, *114*, A02215, doi:10.1029/2008JA013826.

Tao, X., J. Bortnik, J. Albert, K. Liu, and R. Thorne (2011), Comparison of quasilinear diffusion coefficients for parallel propagating whistler mode waves with test particle simulations, *Geophys. Res. Lett.*, *38*, L06105, doi:10.1029/2011GL046787.

Tao, X., J. Bortnik, J. M. Albert, and R. M. Thorne (2012), Comparison of bounce-averaged quasi-linear diffusion coefficients for parallel propagating whistler mode waves with test particle simulations, *J. Geophys. Res.*, *117*, A10205, doi:10.1029/2012JA017931.

Tautz, R., A. Shalchi, and R. Schlickeiser (2008), Solving the 90° scattering problem in isotropic turbulence, *Astrophys. J. Lett.*, *685*, L165, doi:10.1086/592498.

Thorne, R. M. (2010), Radiation belt dynamics: The importance of wave-particle interactions, *Geophys. Res. Lett.*, *37*, L22107, doi:10.1029/2010GL044990.

Thorne, R. M., et al. (2013), Rapid local acceleration of relativistic radiation-belt electrons by magnetospheric chorus, *Nature*, *504*(7480), 411–414.

Tu, W., X. Li, Y. Chen, G. D. Reeves, and M. Temerin (2009), Storm-dependent radiation belt electron dynamics, *J. Geophys. Res.*, *114*, A02217, doi:10.1029/2008JA013480.

Tu, W., G. Cunningham, Y. Chen, M. Henderson, E. Camporeale, and G. Reeves (2013), Modeling radiation belt electron dynamics during GEM challenge intervals with the DREAM3 diffusion model, *J. Geophys. Res. Space Physics*, *118*, 6197–6211, doi:10.1002/jgra.50560.

Varotsou, A., D. Boscher, S. Bourdarie, R. B. Horne, N. P. Meredith, S. A. Glauert, and R. H. Friedel (2008), Three-dimensional test simulations of the outer radiation belt electron dynamics including electron-chorus resonant interactions, *J. Geophys. Res.*, *113*, A12212, doi:10.1029/2007JA012862.

Xiao, F. (2006), Modelling energetic particles by a relativistic kappa-loss-cone distribution function in plasmas, *Plasma Phys. Control. Fusion*, *48*(2), 203, doi:10.1088/0741-3335/48/2/003.

Xiao, F., C. Shen, Y. Wang, H. Zheng, and S. Wang (2008), Energetic electron distributions fitted with a relativistic kappa-type function at geosynchronous orbit, *J. Geophys. Res.*, *113*, A05203, doi:10.1029/2007JA012903.

Xiao, F., Z. Su, H. Zheng, and S. Wang (2009), Modeling of outer radiation belt electrons by multidimensional diffusion process, *J. Geophys. Res.*, *114*, A03201, doi:10.1029/2008JA013580.

Xiao, F., Z. Su, H. Zheng, and S. Wang (2010), Three-dimensional simulations of outer radiation belt electron dynamics including cross-diffusion terms, *J. Geophys. Res.*, *115*, A05216, doi:10.1029/2009JA014541.